

The precession of orbital plane and the significant variabilities of binary pulsars

Biping Gong

Department of Astronomy, Nanjing University, Nanjing 210093, PR. China

bpcheng@nju.edu.cn

ABSTRACT

There are two kinds of expressions on the precession of orbital plane of a binary pulsar system, which are given by Barker & O'Connell (1975) and Apostolatos et al. (1994), Kidder (1995) respectively. This paper analyzes that the former one is obtained in the case of 12 degrees of freedom to a binary pulsar system; whereas the latter one corresponds to 9 degrees of freedom. Consequently the former expression is inconsistent with the conservation of the total angular momentum vector; whereas the latter one is consistent with it. This is Analogous to the calculation of the motion of a small mass at the bottom of a clock pendulum, if we assume that the degree of freedom of this small mass is 2, then this small mass can move every in the 2-dimension space, and the length of the pendulum is not a constant. On the other hand once the length of the pendulum is a constant, the degree of freedom is 1 instead of 2. Damour & Schäfer (1988) and Wex & Kopeikin (1999) has applied Barker & O'Connell's orbital precession velocity in pulsar timing measurement. This paper applies Apostolatos et al. & Kidder's orbital precession velocity in pulsar timing measurement. We analyze that Damour & Schäfer's treatment corresponds to negligible Spin-Orbit induced precession of periastron. Whereas the effects corresponding to Wex & Kopeikin and this paper are both significant (however they are not equivalent). The observational data of two typical binary pulsars support significant Spin-Orbit induced effect, but the validity of the predictions given by Wex & Kopeikin and this paper needs further test on specific binary pulsars with orbital plane nearly edge on.

Subject headings: pulsars: binary pulsars, geodetic precession

1. Introduction

In the gravitational two-body problem with spin, each body is precessing in the gravitational field of its companion, with precession velocity of 1 Post-Newtonian order (PN) (Barker & O'Connell 1975, hereafter BO). This precession velocity is widely accepted. But how does the orbital plane react to the torque caused by the precession of the two bodies has two kinds of treatments. BO's orbital precession velocity is obtained by assuming that the angular momentum vector, \mathbf{L} , precesses at the same velocity as the Runge-Lenz vector, \mathbf{A} .

On the other hand, in the study of the modulation of the gravitational wave by Spin-Orbit (S-L) coupling effect on merging binaries (Apostolatos et al. 1994, Kidder 1995, hereafter AK) obtain an orbital precession velocity that satisfies the conservation of the total angular momentum, \mathbf{J} , and the triangle constraint, $\mathbf{J} = \mathbf{L} + \mathbf{S}$ (where \mathbf{S} is the sum of spin angular momenta of two bodies, \mathbf{S}_1 and \mathbf{S}_2).

The discrepancy in the assumptions leads to different behaviors in physics between BO and AK's orbital precession velocities. The former isn't consistent with the triangle constraint, whereas the latter is. And the reason of this discrepancy is that the former assumes that the four vectors, \mathbf{S}_1 , \mathbf{S}_2 , \mathbf{r}_1 and \mathbf{r}_2 (\mathbf{r}_1 , \mathbf{r}_2 are position vectors of the two bodies respectively), are independent, and the degree of freedom of the binary system is 12; whereas, the latter actually assumes that the independent vectors are either \mathbf{S}_1 , \mathbf{r}_1 and \mathbf{r}_2 ; or \mathbf{S}_2 , \mathbf{r}_1 and \mathbf{r}_2 . And the degree of freedom is 9.

The discrepancy between BO and AK's precession velocities is similar to the following case. The motion of a small mass at the bottom of a clock pendulum can be described in $x - y$ plane. However if we treat the degree of freedom of this small mass as 2, then this small mass can move every in the 2-dimension space, and the length of the pendulum is not a constant. In other words, once the length of the pendulum is a constant, the degree of freedom is 1 instead of 2. Correspondingly if the degree of freedom of a binary system is 12, as treated by BO, then the triangle constraint cannot be satisfied (or \mathbf{J} cannot be a constant vector). On the other hand, if the triangle constraint is satisfied, the degree of freedom cannot be 12, instead it is 9.

In the application to pulsar timing measurement, BO's orbital precession velocity is treated in two different ways, by Damour & Schäfer (1988) and Wex & Kopeikin (1999) respectively. The former one predicts insignificant S-L coupling induced precession of periastron, $\dot{\omega}^S$, and the derivative of orbital period, \dot{P}_b , whereas the latter predicts significant $\dot{\omega}^S$ and \dot{P}_b . The reason is that Damour & Schäfer and Wex & Kopeikin calculated in different kinds of coordinate systems, the former coordinate system is not at rest to "an observer" at the Solar System Baryon center (SSB), whereas, the latter is at rest to it.

If we apply AK's orbital precession velocity to pulsar timing measurement, and calculates S-L coupling induced effect in the same coordinate system as that of Wex & Kopeikin (1999), then significant $\dot{\omega}^S$ and \dot{P}_b are given, but they are not equivalent to the ones that given by Wex & Kopeikin (1999). The validity of these two expressions can be tested by specific binary pulsars with orbital inclination close to $\pi/2$.

This paper contains three parts: (a) the physical discrepancy between BO and AK's orbital precession velocity (Sect 2,3); (b) the derivation of S-L coupling induced effect corresponding to AK's expression of orbital precession (Sect 4,5); (c) the discrepancy between the coordinate systems used by Damour & Schäfer (1988) and Wex & Kopeikin (1999), as well as the relationships among three kinds of S-L coupling induced effects, Damour & Schäfer and Wex & Kopeikin and this paper (Sect 6,7,8).

2. Orbital precession velocity

This section introduces the derivation of the orbital precession velocity of BO and AK.

2.1. Derivation of BO's orbital precession velocity

BO's two-body equation was the first gravitational two-body equation with spin, which consists of two parts, the precession velocity of the spin angular momenta vectors of body one and body two, and the precession velocity of the orbital angular momentum vector. Body one precesses in the gravitational field of body two, with precession velocity (BO),

$$\dot{\Omega}_1 = \frac{L(4 + 3m_2/m_1)}{2r^3} \hat{\mathbf{L}} + \frac{S_2}{2r^3} [\hat{\mathbf{S}}_2 - 3(\hat{\mathbf{L}} \cdot \hat{\mathbf{S}}_2) \hat{\mathbf{L}}] \quad (1)$$

where $\hat{\mathbf{L}}$, $\hat{\mathbf{S}}_1$ and $\hat{\mathbf{S}}_2$ are unit vectors of the orbital angular momentum, the spin angular momentum of star 1 and star 2, respectively.

$\dot{\Omega}_2$ can be obtained by exchanging the subscript 1 and 2 at the right side of Eq.(1). The first term of Eq.(1) represents the geodetic (de Sitter) precession, which corresponds to the precession of \mathbf{S}_1 around \mathbf{L} , it is 1PN due to $\frac{L}{r^3} \sim (\frac{v}{c})^2(\frac{v}{r})$; and the second term represents the Lense-Thirring precession, \mathbf{S}_1 around \mathbf{S}_2 , which is $\frac{S}{L}$ times smaller than the first, therefore, it corresponds to 1.5PN. The the precession velocity of the spin angular momenta vectors is confirmed by other authors using different method.

However for the precession velocity of the orbit, there are different expressions. BO's orbital precession velocity is given as follows.

The total Hamiltonian for the gravitational two-body problem with spin is given (BO, Damour & Schäfer 1988),

$$H = H_N + H_{1PN} + H_{2PN} + H_S, \quad (2)$$

where H_N , H_{1PN} and H_{2PN} are the Newtonian, the first and second order post-Newtonian terms respectively. H_S is the spin-orbit interaction Hamiltonian (BO, Damour & Schäfer 1988),

$$H_S = \sum_{\alpha=1}^2 (2 + 3\frac{m_{\alpha+1}}{m_{\alpha}}) \left(\frac{\mathbf{S}_{\alpha} \cdot \mathbf{L}}{r^3} \right), \quad (3)$$

where $\alpha + 1$ is meant modulo 2 (2+1=1), m_1 , m_2 are the masses of the two stars, respectively, $r = a(1-e^2)^{1/2}$, a is the semi-major axis, e is the eccentricity of the orbit. Notice we uses $G = c = 1$ until discussing observational effects in Sec 5 to Sec 7.

The BO equation describes the secular effect of the orbital plane by a rotational velocity vector, $\dot{\Omega}_S$, acting on some instantaneous Newtonian ellipse. Damour & Schäfer (1988) computed $\dot{\Omega}_S$ in a simple manner by making full use of the Hamiltonian method. The functions of the canonically

conjugate phase space variables \mathbf{r} and \mathbf{p} are defined as

$$\mathbf{L}(\mathbf{r}, \mathbf{p}) = \mathbf{r} \times \mathbf{p} , \quad (4)$$

$$\mathbf{A}(\mathbf{r}, \mathbf{p}) = \mathbf{p} \times \mathbf{L} - GM\mu^2 \frac{\mathbf{r}}{r} , \quad (5)$$

where $\mathbf{r} = \mathbf{r}_1 - \mathbf{r}_2$, $M = m_1 + m_2$, $\mu = m_1 m_2 / M$. The vector \mathbf{A} is the Runge-Lenz vector (first discovered by Lagrange). The instantaneous Newtonian ellipse evolves according to the fundamental equations of Hamiltonian dynamics (Damour & Schäfer 1988)

$$\dot{\mathbf{L}} = \{\mathbf{L}, H\} , \quad (6)$$

$$\dot{\mathbf{A}} = \{\mathbf{A}, H\} , \quad (7)$$

where $\{\cdot, \cdot\}$ denote the Poisson bracket. \mathbf{L} and \mathbf{A} are first integrals of H_N , only $H_{1PN} + H_{2PN} + H_S$ contributes to the right-hand sides of Eq.(6) and Eq.(7), in which $H_{1PN} + H_{2PN}$ determines the precession of periastron, in 1PN it is given,

$$\dot{\omega}^{GR} = \frac{6\pi M}{P_b a(1 - e^2)} , \quad (8)$$

where P_b is the orbital period. To study the spin-orbit interaction, it is sufficient to consider H_S . Thus replacing H of Eq.(6) and Eq.(7) by H_S obtains (Damour & Schäfer 1988),

$$(\frac{d\mathbf{L}}{dt})_S = \{\mathbf{L}, H_S\} = \dot{\Omega}_S^* \hat{\mathbf{S}} \times \mathbf{L} , \quad (9)$$

$$(\frac{d\mathbf{A}}{dt})_S = \{\mathbf{A}, H_S\} = \dot{\Omega}_S^* [\hat{\mathbf{S}} - 3(\hat{\mathbf{L}} \cdot \hat{\mathbf{S}})\hat{\mathbf{L}}] \times \mathbf{A} . \quad (10)$$

where

$$\dot{\Omega}_S^* = \frac{S(4 + 3m_2/m_1)}{2r^3} . \quad (11)$$

By Damour & Schäfer (1988), \mathbf{S} represents a linear combination of \mathbf{S}_1 and \mathbf{S}_2 . For simplicity of discussion, and for consistence with Wex & Kopeikin's application of $\dot{\Omega}_S$ (Wex & Kopeikin 1999), we assume $\mathbf{S} = \mathbf{S}_1$ (the other spin angular momentum is ignored) until Sec 4 where the general binary pulsar is discussed.

The solution of Eq.(9) and Eq.(10) gives the S-L coupling induced orbital precession velocity (Damour & Schäfer 1988)

$$\dot{\Omega}_S = \dot{\Omega}_S^* [\hat{\mathbf{S}} - 3(\hat{\mathbf{L}} \cdot \hat{\mathbf{S}})\hat{\mathbf{L}}] . \quad (12)$$

By Eq.(9) and Eq.(12), the first derivative of $\hat{\mathbf{L}}$ can be obtained,

$$\frac{d\hat{\mathbf{L}}}{dt} = \dot{\Omega}_S^* \hat{\mathbf{S}} \times \hat{\mathbf{L}} , \quad (13)$$

and by Eq.(1) the first derivative of $\hat{\mathbf{S}}$ (recall $\mathbf{S} = \mathbf{S}_1$) can be written

$$\frac{d\hat{\mathbf{S}}}{dt} = \dot{\Omega}_1^* \hat{\mathbf{L}} \times \hat{\mathbf{S}} = \Omega_S^* \frac{L}{S} \hat{\mathbf{L}} \times \hat{\mathbf{S}} , \quad (14)$$

where $\dot{\Omega}_1^*$ is the first term at the right hand side of Eq.(1). By Eq.(13) and Eq.(14) $\hat{\mathbf{L}}$ precesses slowly around $\hat{\mathbf{S}}$, 1.5PN, as shown by Eq.(13); whereas $\hat{\mathbf{S}}$ precesses rapidly around $\hat{\mathbf{L}}$, 1PN, as shown in Eq.(14). Therefore the BO equation predicts such a scenario that the two vectors, $\hat{\mathbf{L}}$ and $\hat{\mathbf{S}}$ precess around each with very different precession velocities (typically one is larger than the other by 3 to 4 orders of magnitude for a general binary pulsar system).

2.2. Orbital precession velocity in the calculation of gravitational waves

In the study of the modulation of precession of orbital plane to gravitational waves, the orbital precession velocity is obtained in a different manner and the result is very different from that given by Eq.(12).

Since the gravitational wave corresponding to 2.5PN, which is negligible compared with S-L coupling effect that corresponds to 1PN and 1.5PN, the total angular momentum can be treated as conserved, $\mathbf{J} = 0$. Then the following equation can be obtained (BO),

$$\dot{\Omega}_0 \times \mathbf{L} = -\dot{\Omega}_1 \times \mathbf{S}_1 - \dot{\Omega}_2 \times \mathbf{S}_2 . \quad (15)$$

Notice that as defined by BO and AK, $\mathbf{L} = \mu M^{1/2} r^{1/2} \hat{\mathbf{L}}$. In the one-spin case the right hand side of Eq.(15) can be given (Kidder 1995),

$$\dot{\mathbf{S}} = \frac{1}{2r^3} \left(4 + \frac{3m_2}{m_1} \right) (\mathbf{L} \times \mathbf{S}) , \quad (16)$$

and considering that $\mathbf{J} = \mathbf{L} + \mathbf{S}$, Eq.(16) can be written,

$$\dot{\mathbf{S}} = \frac{1}{2r^3} \left(4 + \frac{3m_2}{m_1} \right) (\mathbf{J} \times \mathbf{S}) . \quad (17)$$

From Eq.(15), $\dot{\mathbf{L}}$ can be given,

$$\dot{\mathbf{L}} = \frac{1}{2r^3} \left(4 + \frac{3m_2}{m_1} \right) (\mathbf{J} \times \mathbf{L}) . \quad (18)$$

By Eq.(17) and Eq.(18), \mathbf{L} and \mathbf{S} precess about the fixed vector \mathbf{J} at the same rate with a precession frequency approximately (AK)

$$\dot{\Omega}_0 = \frac{\mathbf{J}}{2r^3} \left(4 + \frac{3m_2}{m_1} \right) . \quad (19)$$

Eq.(19) indicates that in the 1 PN approximation, $\hat{\mathbf{L}}$ and $\hat{\mathbf{S}}$ can precess around \mathbf{J} rapidly (1PN) with exactly the same velocity. Notice that the misalignment angles between $\hat{\mathbf{L}}$ and $\hat{\mathbf{S}}$ (λ_{LS}), $\hat{\mathbf{L}}$ and $\hat{\mathbf{J}}$ (λ_{LJ}) are very different, due to $S/L \ll 1$, λ_{LJ} is much smaller than λ_{LS} .

Thus, AK's equations, Eq.(18) and Eq.(17), correspond to a very different scenario of motion of \mathbf{S} , \mathbf{L} and \mathbf{J} from that given by BO equation shown in Eq.(13) and Eq.(14).

3. Physical differences between BO and AK

This section compares two different scenarios corresponding to BO and AK's orbital precession velocity, and points out that BO's orbital precession velocity is actually inconsistent with the definition of the total angular momentum of a binary system.

Section 2 indicates that BO and AK derived the orbital precession velocity in different ways, therefore two different orbital precession velocity vectors are obtained, as shown in Eq.(12) and Eq.(19), respectively, which in turn correspond to different scenarios of motion of the three vectors. This section analyzes that the discrepancy between BO and AK is not just a discrepancy corresponding to different coordinate systems. Actually there is significant physical differences between BO and AK. The total angular momentum of a binary system is defined as BO

$$\mathbf{J} = \mathbf{L} + \mathbf{S} , \quad (20)$$

Eq.(20) means that \mathbf{J} , \mathbf{L} and \mathbf{S} form a triangle, and therefore, it guarantees that the three vectors must be in one plane at any moment. For a general radio binary pulsar system, the total angular momentum of this system is conserved in 1PN. Therefore we have

$$\dot{\mathbf{J}} = 0 . \quad (21)$$

Eq.(21) means that \mathbf{J} is a constant during the motion of a binary system. Eq.(21) and Eq.(20) together provide a scenario that the triangle formed by \mathbf{L} , \mathbf{S} and \mathbf{J} determines a plane, and the plane rotates around a fixed axis, \mathbf{J} , with velocity $\dot{\Omega}_0$. This scenario is shown in Fig 1. which can also be represented as

$$\dot{\mathbf{J}} = \dot{\Omega}_0 \hat{\mathbf{J}} \times \mathbf{L} + \dot{\Omega}_0 \hat{\mathbf{J}} \times \mathbf{S} = 0 , \quad (22)$$

Smarr & Blandford (1976) mentioned the scenario that \mathbf{L} and \mathbf{S} must be at opposite side of \mathbf{J} at any instant. Hamilton and Sarazin (1982) also study the scenario and state that \mathbf{L} precesses rapidly around \mathbf{J} . Obviously the orbital precession velocity given by Eq.(19) can satisfy the two constraints, Eq.(20) and Eq.(21) simultaneously.

Can the BO's orbital precession velocity given by Eq.(12) satisfy the two constraints, Eq.(20) and Eq.(21) simultaneously ? From Eq.(12), Eq.(13) and Eq.(14), the first derivative of \mathbf{J} can be written (BO)

$$\dot{\mathbf{J}} = \dot{\Omega}_S \times \mathbf{L} + \dot{\Omega}_1^* \times \mathbf{S} = \dot{\Omega}_S^* \hat{\mathbf{S}} \times \mathbf{L} + \dot{\Omega}_1^* \hat{\mathbf{L}} \times \mathbf{S} \equiv 0 , \quad (23)$$

and since Eq.(20) is defined in BO's equation, then it seems that the BO equation can satisfy both Eq.(20) and Eq.(21).

But in BO's derivation of $\dot{\Omega}_S$ (Eq.(6)–Eq.(12)), Eq.(20) is never used. The corresponding $\dot{\Omega}_S$ can make $\dot{\mathbf{J}} = \dot{\mathbf{L}} + \dot{\mathbf{S}} \equiv 0$, as shown in Eq.(23), however it cannot guarantee that $\mathbf{J} = \mathbf{L} + \mathbf{S}$ is satisfied. In other words, when $\mathbf{J} \neq \mathbf{L} + \mathbf{S}$, Eq.(23) is still correct. This can be easily tested by putting $\mathbf{L}' = \mathbf{L} + \alpha \mathbf{S}$, or $\mathbf{S}' = \mathbf{S} + \beta \mathbf{L}$ (α and β are arbitrary constants) into Eq.(23) to replace \mathbf{L} and \mathbf{S} , respectively, obviously in such cases, Eq.(23) is still satisfied ($\dot{\mathbf{J}} \equiv 0$).

Contrarily in AK's derivation of $\dot{\Omega}_0$ (Eq.(16)–Eq.(18)), the relation Eq.(20) is used. And if we do the same replacement of $\mathbf{L}' = \mathbf{L} + \alpha \mathbf{S}$, or $\mathbf{S}' = \mathbf{S} + \beta \mathbf{L}$ in Eq.(22), then Eq.(22) is violated ($\dot{\mathbf{J}} \neq 0$). This means that for AK's $\dot{\Omega}_0$, if Eq.(20) is violated then Eq.(21) is violated also. Thus in AK's expression, the conservation of the total angular momentum is dependent on Eq.(20), whereas, in BO's expression, the conservation of the total angular momentum is independent of Eq.(20). If we rewrite Eq.(20) as,

$$\mathbf{J} = \mathbf{L} + \mathbf{S} + \mathbf{C}, \quad (24)$$

then in BO's expression, the conservation of the total angular momentum can be satisfied in the case that $\mathbf{C} \neq 0$ in Eq.(24); whereas, in AK's expression, the conservation of the total angular momentum is satisfied only when $\mathbf{C} = 0$ in Eq.(24). This means that the discrepancy between BO and AK's orbital precession velocity is physical. It is not just different expression in different coordinate systems or relative to different directions.

Moreover Eq.(22) and Eq.(19) correspond to the following orbital precession velocity,

$$\dot{\Omega}_0 = \dot{\Omega}_S^* (\hat{\mathbf{S}} + \frac{L}{S} \hat{\mathbf{L}}). \quad (25)$$

Obviously Eq.(25) is not consistent with BO's Eq.(12), which demands that the coefficient of the component along $\hat{\mathbf{L}}$ be $\gamma = -3(\hat{\mathbf{L}} \cdot \hat{\mathbf{S}})$, instead of $\gamma = \frac{L}{S}$ as given by Eq.(25).

In other words, once Eq.(20) is satisfied, BO's orbital precession velocity of Eq.(12) must be violated. Therefore, BO's orbital precession velocity cannot be consistent with BO's definition, $\mathbf{J} = \mathbf{L} + \mathbf{S}$.

Actually Eq.(25) can be consistent with Eq.(9), however it is contradictory to Eq.(10). The reason of introducing Eq.(10) is that without it, Eq.(9) alone cannot determine a unique solution.

Whereas, Eq.(22) and Eq.(19) can be regarded as solving this problem by using Eq.(9) and Eq.(20) instead of Eq.(9) and Eq.(10) to obtain the orbital precession velocity.

As defined in Eq.(4) and Eq.(5), \mathbf{L} and \mathbf{A} are vectors that are determined by different elements in celestial mechanics, $\mathbf{L}(\Omega, i)$ and $\mathbf{A}(\Omega, i, \omega, e)$ respectively. And these two vectors satisfy different physical constraints, i.e., \mathbf{L} satisfies Eq.(20) and Eq.(21), whereas, \mathbf{A} doesn't satisfy these two constraints.

Therefore, it is conceivable that \mathbf{L} and \mathbf{A} should correspond to different precession velocities, as given by Eq.(9) and Eq.(10), respectively. However since the discrepancy is only in the $\hat{\mathbf{L}}$ component, which does not influence the satisfaction of the conservation equation, Eq.(23), thus the discrepancy seems unimportant. And therefore, the precession velocity of \mathbf{L} is treated equivalently to that of \mathbf{A} 's, thus the components in $\hat{\mathbf{L}}$ are both treated as $\gamma = -3(\hat{\mathbf{L}} \cdot \hat{\mathbf{S}})$. Whereas, as given by Eq.(25), $\hat{\mathbf{L}}$ component must be $\gamma = \frac{L}{S}$ if the triangle constraint is to be satisfied. Therefore, the violation of the triangle constraint is inevitable under the assumption that \mathbf{L} and \mathbf{A} precess at the same velocity.

4. S-L coupling induced effects derived under different degree of freedom

As analyzed in Sect 2 and Sect 3, whether the triangle constraint is satisfied or not results discrepancy in the orbital precession velocity. This section further analyzes that it is the discrepancy in degree of freedom used by BO and AK that leads to the violation or satisfaction of the triangle constraint.

To discuss the S-L coupling induced effects on observational parameters, one need to obtain the variation of the six orbital elements under S-L coupling. The way of doing this is from the Hamiltonian (corresponding to S-L coupling) to equation of motion, and then through perturbation methods in celestial mechanics to obtain S-L coupling induced effects to observer. In this section this process is performed in the case that the degree of freedom of a binary system (with two spins) is 9, in which the triangle constraint is satisfied.

It is convenient to study the motion of a binary system in such a coordinate system (J-coordinate system), in which the total angular momentum, \mathbf{J} is along the z-axes and the invariance plane is in the x-y plane. The J-coordinate system has two advantages.

- (a) Once a binary pulsar system is given, λ_{LJ} , the misalignment angle between \mathbf{J} and \mathbf{L} , can be estimated, from which $\dot{\Omega}$ and $\dot{\omega}$ can be obtained easily in the J-coordinate system, which are intrinsic to a binary pulsar system.
- (b) Moreover, the J-coordinate system is static relative to the line of sight (after counting out the proper motion). Therefore transforming parameters obtained in the J-coordinates system to observer's coordinate system, S-L coupling induced effects can be obtained reliably.

From Eq.(3), the S-L coupling induced H_S contains potential part only, therefore we have $H_S = U$, where

$$U = U_1 + U_2 = \frac{1}{r^3} (2\mathbf{S} + \frac{3m_2}{2m_1}\mathbf{S}_1 + \frac{3m_1}{2m_2}\mathbf{S}_2) \cdot \mathbf{L} , \quad (26)$$

which can be written as

$$U = \frac{1}{r^3} (\sigma_1 \mathbf{S} \cdot \mathbf{L} + \sigma_2 \mathbf{S}_2 \cdot \mathbf{L}) , \quad (27)$$

where

$$\sigma_1 = 2 + \frac{3}{2} \frac{m_2}{m_1} , \quad \sigma_2 = 2 + \frac{3}{2} \left(\frac{m_1}{m_2} - \frac{m_2}{m_1} \right) . \quad (28)$$

The acceleration is given by

$$\mathbf{a}_{so} = -\nabla U = -\sigma_1 \nabla \frac{(\mathbf{S} \cdot \mathbf{L})}{r^3} - \sigma_2 \nabla \frac{(\mathbf{S}_2 \cdot \mathbf{L})}{r^3} , \quad (29)$$

where, ∇ represents gradient. In the first term at the right hand side of Eq.(29), \mathbf{S} is given by $\mathbf{S} = \mathbf{S}_1 + \mathbf{S}_2$, which is determined by $S_1^{(i)}$ and $S_2^{(i)}$ ($i = 1, 2, 3$). And \mathbf{L} is dependent of \mathbf{r} (recall $\mathbf{r} = \mathbf{r}_1 - \mathbf{r}_2$ and $r_1^{(i)}, r_2^{(i)}$ ($i = 1, 2, 3$) are positions of the two bodies respectively).

Thus the independent variables of Eq.(29) seems $4 \times 3 = 12$. However, by the triangle constraint and the conservation of \mathbf{J} given by Eq.(20) and Eq.(21), we have $\mathbf{J} = \mathbf{L} + \mathbf{S} = \mathbf{L} + \mathbf{S}_1 + \mathbf{S}_2 = \text{const}$

vector, which means that \mathbf{S} and \mathbf{L} are dependent, in other words, these 12 variables are not independent in 1PN approximation.

If we directly calculate Eq.(29) by 12 independent variables then $\mathbf{J} = \text{constant}$ vector must be violated, which is like calculating the motion of a clock pendulum by 2 independent variables, from which the length of the pendulum must be variable, in other words, the constraint that length=constant must be violated in a clock pendulum.

A simple treatment can guarantee that $\mathbf{J} = \text{constant}$ vector be satisfied. That is replacing \mathbf{S} in the equation of motion of Eq.(29) by $\mathbf{J} - \mathbf{L}$. Thus the independent variables can either be $S_2^{(i)}, r_1^{(i)}$ and $r_2^{(i)}$; or $S_1^{(i)}, r_1^{(i)}$ and $r_2^{(i)}$ by different σ_1 and σ_2 from Eq.(27) and Eq.(28), in which the degree of freedom is 9 instead of 12. Thus Eq.(29) can be re-written

$$\nabla \frac{(\mathbf{S} \cdot \mathbf{L})}{r^3} = \nabla \frac{[(\mathbf{J} - \mathbf{L}) \cdot \mathbf{L}]}{r^3} = \nabla \frac{(\mathbf{J} \cdot \mathbf{L})}{r^3} - \nabla \frac{(\mathbf{L} \cdot \mathbf{L})}{r^3} , \quad (30)$$

where

$$\nabla \frac{(\mathbf{J} \cdot \mathbf{L})}{r^3} = -3 \frac{(\mathbf{L} \cdot \mathbf{J})\mathbf{r}}{r^5} - 3 \frac{(\mathbf{J} \times \mathbf{r})(\mathbf{V} \cdot \mathbf{r})}{r^5} \mu + 2 \frac{(\mathbf{J} \times \mathbf{V})}{r^3} \mu , \quad (31)$$

$$\nabla \frac{(\mathbf{L} \cdot \mathbf{L})}{r^3} = -3 \frac{(\mathbf{L} \cdot \mathbf{L})\mathbf{r}}{r^5} - 2 \frac{(\mathbf{L} \times \mathbf{V})}{r^3} \mu , \quad (32)$$

where \mathbf{V} is the velocity of the reduced mass. Put Eq.(31) and Eq.(32) into Eq.(30) and finally into Eq.(29), we have,

$$\begin{aligned} \mathbf{a}_{so} = & \frac{3}{r^3} [\sigma_1 (\mathbf{J} - \mathbf{L}) \cdot (\hat{\mathbf{n}} \times \mathbf{V}) \hat{\mathbf{n}} + \sigma_2 \mathbf{S}_2 \cdot (\hat{\mathbf{n}} \times \mathbf{V}) \hat{\mathbf{n}}] \\ & + \frac{2}{r^3} [2\sigma_1 (\mathbf{V} \times \mathbf{J}) - \sigma_1 (\mathbf{V} \times (\mathbf{J} - \mathbf{L})) + \sigma_2 (\mathbf{V} \times \mathbf{S}_2)] \\ & + \frac{3(\mathbf{V} \cdot \hat{\mathbf{n}})}{r^3} [\sigma_1 (\mathbf{J} \times \hat{\mathbf{n}}) + \sigma_2 (\mathbf{S}_2 \times \hat{\mathbf{n}})] , \end{aligned} \quad (33)$$

where $\hat{\mathbf{n}}$ is the unit vector of \mathbf{r} . Replacing $\mathbf{J} - \mathbf{L}$ by \mathbf{S} , Eq.(33) can be written,

$$\begin{aligned} \mathbf{a}_{so} = & \frac{3}{r^3} [\sigma_1 \mathbf{S} \cdot (\hat{\mathbf{n}} \times \mathbf{V}) \hat{\mathbf{n}} + \sigma_2 \mathbf{S}_2 \cdot (\hat{\mathbf{n}} \times \mathbf{V}) \hat{\mathbf{n}}] \\ & + \frac{2}{r^3} [2\sigma_1 (\mathbf{V} \times \mathbf{J}) - \sigma_1 (\mathbf{V} \times \mathbf{S}) + \sigma_2 (\mathbf{V} \times \mathbf{S}_2)] \\ & + \frac{3(\mathbf{V} \cdot \hat{\mathbf{n}})}{r^3} [\sigma_1 (\mathbf{J} \times \hat{\mathbf{n}}) + \sigma_2 (\mathbf{S}_2 \times \hat{\mathbf{n}})] . \end{aligned} \quad (34)$$

If one calculates \mathbf{a}_{so} directly by Eq.(29) without imposing the triangle constraint, then the corresponding result can be given by replacing \mathbf{J} of Eq.(34) by \mathbf{S} ,

$$\begin{aligned} \mathbf{a}'_{so} = & \frac{3}{r^3} [\sigma_1 \mathbf{S} \cdot (\hat{\mathbf{n}} \times \mathbf{V}) \hat{\mathbf{n}} + \sigma_2 \mathbf{S}_2 \cdot (\hat{\mathbf{n}} \times \mathbf{V}) \hat{\mathbf{n}}] \\ & + \frac{2}{r^3} [\sigma_1 (\mathbf{V} \times \mathbf{S}) + \sigma_2 (\mathbf{V} \times \mathbf{S}_2)] \end{aligned}$$

$$+ \frac{3(\mathbf{V} \cdot \hat{\mathbf{n}})}{r^3} [\sigma_1(\mathbf{S} \times \hat{\mathbf{n}}) + \sigma_2(\mathbf{S}_2 \times \hat{\mathbf{n}})] . \quad (35)$$

Notice that Eq.(35) is equivalent to the sum of Eq.(52) and Eq.(53) given by the BO equation. The difference between Eq.(34) and Eq.(35) indicates that whether the triangle constraint is satisfied or not (9 or 12 degree of freedom) can lead to significant differences in \mathbf{a}_{so} , which in turn results in significant differences on the predictions of observational effects as discussed in the next section.

Having \mathbf{a}_{so} , we can use the standard method in celestial mechanics to calculate,

$$\tilde{S} = \mathbf{a}_{so} \cdot \hat{\mathbf{n}}, \quad \tilde{T} = \mathbf{a}_{so} \cdot \hat{\mathbf{t}}, \quad \tilde{W} = \mathbf{a}_{so} \cdot \hat{\mathbf{L}}, \quad (36)$$

from which one can calculate the derivative of the six orbit elements and then transform to the observer's coordinate system to compare with observation. The unit vector, $\hat{\mathbf{n}}$, in Eq.(34) to Eq.(36) is given by,

$$\hat{\mathbf{n}} = \mathbf{P} \cos f + \mathbf{Q} \sin f , \quad (37)$$

and $\hat{\mathbf{t}}$ is the unit vector that is perpendicular to $\hat{\mathbf{n}}$,

$$\hat{\mathbf{t}} = -\mathbf{P} \sin f + \mathbf{Q} \cos f , \quad (38)$$

and $\mathbf{V} = \mathbf{p}/\mu$, is given by

$$\mathbf{V} = -\frac{h}{p} \mathbf{P} \cos f + \frac{h}{p} \mathbf{Q} (e + \cos f) , \quad (39)$$

where f is the true anomaly, p is the semilatus rectum, $p = a(1 - e^2)$, and h is the integral of area, $h = r^2 \dot{f}$. \mathbf{P} is given by three components,

$$\begin{aligned} P_x &= \cos \Omega \cos \omega - \sin \Omega \sin \omega \cos \lambda_{LJ} , \\ P_y &= \sin \Omega \cos \omega + \cos \Omega \sin \omega \cos \lambda_{LJ} , \\ P_z &= \sin \omega \sin \lambda_{LJ} , \end{aligned} \quad (40)$$

and \mathbf{Q} is given by three components,

$$\begin{aligned} Q_x &= -\cos \Omega \sin \omega - \sin \Omega \cos \omega \cos \lambda_{LJ} , \\ Q_y &= -\sin \Omega \sin \omega + \cos \Omega \cos \omega \cos \lambda_{LJ} , \\ Q_z &= \cos \omega \sin \lambda_{LJ} , \end{aligned} \quad (41)$$

The unit vector of $\hat{\mathbf{L}}$ and $\hat{\mathbf{S}}_\kappa$ ($\kappa = 1, 2$) are given,

$$\hat{\mathbf{L}} = (\sin \lambda_{LJ} \cos \eta_L, \sin \lambda_{LJ} \sin \eta_L, \cos \lambda_{LJ})^T , \quad (42)$$

$$\hat{\mathbf{S}}_\kappa = (\sin \lambda_{JS\kappa} \cos \eta_{S\kappa}, \sin \lambda_{JS\kappa} \sin \eta_{S\kappa}, \cos \lambda_{JS\kappa})^T . \quad (43)$$

In the perturbation equation, the acceleration of Eq.(34), \mathbf{a}_{so} , is expressed along $\hat{\mathbf{n}}$, $\hat{\mathbf{t}}$ and $\hat{\mathbf{L}}$ respectively. We can use \mathbf{a}_1 , \mathbf{a}_2 and \mathbf{a}_3 to represent terms corresponding to the three terms containing brackets $[,]$ at the right hand side of Eq.(34), respectively. Projecting \mathbf{a}_1 onto $\hat{\mathbf{L}}$, we have

$$W_1 = \mathbf{a}_1 \cdot \hat{\mathbf{L}} = \frac{3\sigma_1}{r^3} [S_x(n_y V_z - n_z V_y) + S_y(n_z V_x - n_x V_z) + S_z(n_z V_y - n_y V_z)] \\ (n_x \sin \lambda_{LJ} \cos \eta_L + n_y \sin \lambda_{LJ} \sin \eta_L + n_z \cos \lambda_{LJ}) , \quad (44)$$

where n_x , n_y , n_z and V_x , V_y , V_z are components of $\hat{\mathbf{n}}$ and \mathbf{V} along axes, x , y and z , respectively. Similarly, projecting \mathbf{a}_2 onto $\hat{\mathbf{L}}$, we have,

$$W_2 = \mathbf{a}_2 \cdot \hat{\mathbf{L}} = \frac{\sigma_1}{r^3} (V_y J \sin \lambda_{LJ} \cos \eta_L - V_x J \sin \lambda_{LJ} \sin \eta_L) \\ + [\frac{\sigma_1}{r^3} (V_x S_y - V_y S_x) + \frac{2\sigma_2}{r^3} (V_x S_{2y} - V_y S_{2x})] \cos \lambda_{LJ} . \quad (45)$$

Finally \mathbf{a}_3 can also be projected onto $\hat{\mathbf{L}}$,

$$W_3 = \mathbf{a}_3 \cdot \hat{\mathbf{L}} = \frac{\cos \lambda_{LJ}}{r^3} [\sigma_1 (V_y^r S_x - V_x^r S_y) + \sigma_2 (V_y^r S_{2x} - V_x^r S_{2y})] , \quad (46)$$

where $V_x^r = 3\dot{r}n_x$, $V_y^r = 3\dot{r}n_y$ and $\dot{r} = \frac{eh}{p} \sin f$. Therefore, the sum of W is

$$\widetilde{W} = W_1 + W_2 + W_3 . \quad (47)$$

The effect around \mathbf{J} can be obtained by perturbation equations (Roy 1991, Yi 1993, Liu 1993) and Eq.(47)

$$\frac{d\Omega}{dt} = \frac{\widetilde{W} r \sin(\omega + f)}{na^2 \sqrt{1 - e^2}} \frac{1}{\sin \lambda_{LJ}} , \quad (48)$$

where n is the angular velocity. Averaging over one orbital period we have

$$\langle \frac{d\Omega}{dt} \rangle = \frac{3 \cos \lambda_{LJ}}{2a^3(1 - e^2)^{3/2} \sin \lambda_{LJ}} [(P_z \sin \omega + Q_x \cos \omega) [(P_y Q_z - P_z Q_y)(S_x \sigma_1 + S_{2x} \sigma_2) \\ + (P_z Q_x - P_x Q_z)(S_y \sigma_1 + S_{2y} \sigma_2) + (P_x Q_y - P_y Q_x)(S_z \sigma_1 + S_{2z} \sigma_2)]] . \quad (49)$$

Notice that the average value of Eq.(49) depends on W_1 only, the contribution of W_2 and W_3 to it is zero. With $S/\sin \lambda_{LJ} \sim L$, we have $d\Omega/dt \sim L/a^3$, which corresponds to 1PN.

The $d\omega/dt$ can be obtained by calculation of $\widetilde{S} = \mathbf{a}_{so} \cdot \hat{\mathbf{n}}$ and $\widetilde{T} = \mathbf{a}_{so} \cdot \hat{\mathbf{t}}$. Since $\mathbf{a}_1 \cdot \hat{\mathbf{n}}$ and $\mathbf{a}_1 \cdot \hat{\mathbf{t}}$ are 1.5PN. Therefore, it is sufficient to consider the projection of \mathbf{a}_2 and \mathbf{a}_3 onto $\hat{\mathbf{n}}$, $\hat{\mathbf{t}}$ respectively, thus we have,

$$\langle (\mathbf{a}_2 \cdot \hat{\mathbf{n}}) \cos f \rangle = \frac{7\sigma_1 J}{8(1 - e^2)^{3/2} a^3} \frac{eh}{p} (P_x Q_y - P_y Q_x) , \quad (50)$$

$$\langle (\mathbf{a}_2 \cdot \hat{\mathbf{t}}) \sin f \rangle = \frac{-\sigma_1 J}{2(1 - e^2)^{3/2} a^3} \frac{eh}{p} (P_x Q_y - P_y Q_x) , \quad (51)$$

$$\langle (\mathbf{a}_3 \cdot \hat{\mathbf{t}}) \sin f \rangle = \frac{-3\sigma_1 J}{2(1-e^2)^{3/2}a^3} \frac{eh}{p} (P_x Q_y - P_y Q_x) , \quad (52)$$

$$\langle (\mathbf{a}_3 \cdot \hat{\mathbf{n}}) \cos f \rangle = 0 . \quad (53)$$

From Eq.(50) to Eq.(53), we have

$$\begin{aligned} \frac{d\omega'}{dt} &= \frac{\sqrt{1-e^2}}{nae} \{ [-\mathbf{a}_2 \cdot \hat{\mathbf{n}}] \cos f + (1 + \frac{r}{p}) [\mathbf{a}_2 \cdot \hat{\mathbf{t}}] \sin f \} \\ &= \frac{7\sigma_1 J}{2(1-e^2)^{3/2}a^3} \frac{eh}{p} (P_y Q_x - P_x Q_y) . \end{aligned} \quad (54)$$

therefore, by the standard perturbation (Roy 1991, Yi 1993, Liu 1993), the advance of precession of periastron induced by S-L coupling is given by

$$\frac{d\omega}{dt} = \frac{d\omega'}{dt} - \frac{d\Omega}{dt} \cos \lambda_{LJ} . \quad (55)$$

By putting Eq.(50) and Eq.(51) into Eq.(55), and averaging over one orbital period we have,

$$\langle \frac{d\omega}{dt} \rangle = \frac{7\sigma_1 J}{2(1-e^2)^{3/2}a^3} \frac{eh}{p} (P_y Q_x - P_x Q_y) - \frac{d\Omega}{dt} \cos \lambda_{LJ} . \quad (56)$$

Using perturbation equations as in (Roy 1991, Yi 1993, Liu 1993), and by Eq.(48) and Eq.(56), we have

$$\begin{aligned} \langle \frac{d\varpi}{dt} \rangle &= \frac{7\sigma_1 J}{2(1-e^2)^{3/2}a^3} \frac{eh}{p} (P_y Q_x - P_x Q_y) + 2 \frac{d\Omega}{dt} \sin^2 \frac{\lambda_{LJ}}{2} \\ &= \frac{7\sigma_1 J}{2(1-e^2)^{3/2}a^3} \frac{eh}{p} (P_y Q_x - P_x Q_y) + O(c^{-3}) . \end{aligned} \quad (57)$$

Eq.(49), Eq.(56) and Eq.(57) indicate that the magnitude of $d\Omega/dt$, and $d\varpi/dt$ are both L/a^3 (1PN), whereas, $d\omega/dt$ can be 1.5PN (or zero in 1PN) by Eq.(56).

$d\Omega/dt$ (1PN) of Eq.(48) is equivalent to $\dot{\Phi}_S$ (1PN) which is given by Wex & Kopeikin (1999). This is because the averaged value of $d\Omega/dt$ depends only on \mathbf{a}_1 , the first term containing bracket $[]$ in \mathbf{a}_{so} , as shown in Eq.(34). And both this paper (\mathbf{a}_{so} of Eq.(34)) and that of BO equation (\mathbf{a}'_{so} of Eq.(35)) give the same \mathbf{a}_1 . Thus, different authors give the equivalent value on the averaged $d\Omega/dt$.

Whereas, $d\omega/dt$ of Eq.(56) and $\dot{\Psi}_S$ (1PN) given by Wex & Kopeikin (1999) are very different in magnitude. The difference is due to the fact that $d\omega/dt$ given by Eq.(56) of this paper is obtained by the \mathbf{a}_{so} of Eq.(34); whereas, the corresponding $d\omega/dt$ of Wex and Kopeikin (1999) is obtained by the \mathbf{a}'_{so} of Eq.(35), which is equivalent of replacing J of Eq.(34) by S .

And in turn, the difference between \mathbf{a}_{so} and \mathbf{a}'_{so} is due to that \mathbf{a}_{so} satisfies the triangle constraint (9 degrees of freedom); whereas \mathbf{a}'_{so} (12 degrees of freedom) doesn't. Therefore, a small difference in the equation of motion causes significant discrepancy in the variation of elements, such as $d\omega/dt$.

5. Effects on $\dot{\omega}$, \dot{x} , \dot{P}_b

As shown in Sect 4 the S-L coupling effect can be treated as a perturbation to the Newtonian two-body problem, and by the standard method in celestial mechanics the variation of six orbital elements can be obtained. This section calculates what $\dot{\omega}$, \dot{x} , \dot{P}_b are for an observer when the variation of the six orbital elements is given. The results of this section is independent of the degree of freedom used in a binary system.

The observational effect is studies in such a coordinate system that the vector \mathbf{K}_0 (corresponding to line of sight) is along the z' -axis; the x' axis is along the intersection of the plane of the sky and the invariance plane; and the y' -axis is perpendicular to $x' - z'$ plane, as shown in Fig 2a. Obviously this coordinate system is at rest to "an observer" at the SSB. The relationship of dynamical longitude of the ascending node, Ω , dynamical longitude of the periastron, ω , and the orbital inclination, i , can be given (Smarr & Blandford 1976, Wex & Kopeikin 1999)

$$\cos i = \cos I \cos \lambda_{LJ} - \sin \lambda_{LJ} \sin I \cos \Omega , \quad (58)$$

and

$$\begin{aligned} \sin i \sin \omega^{\text{obs}} &= (\cos I \sin \lambda_{LJ} + \cos \lambda_{LJ} \sin I \cos \Omega) \sin \omega \\ &\quad + \sin I \sin \Omega \cos \omega , \end{aligned} \quad (59)$$

$$\begin{aligned} \sin i \cos \omega^{\text{obs}} &= (\cos I \sin \lambda_{LJ} + \cos \lambda_{LJ} \sin I \cos \Omega) \cos \omega \\ &\quad - \sin I \sin \Omega \sin \omega , \end{aligned} \quad (60)$$

where I is the misalignment angle between \mathbf{J} and the line of sight. The semi-major axis of the pulsar is defined as

$$x \equiv \frac{a_p \sin i}{c} . \quad (61)$$

where a_p is the semi-major axis of the pulsar. By Eq.(58), we have,

$$\dot{x}_1 = \frac{a_p \cos i}{c} \frac{di}{dt} = -x \dot{\Omega} \sin \lambda_{LJ} \sin \Omega \cot i . \quad (62)$$

The semi-major axis of the orbit is $a = \frac{M}{m_2} a_p$, and since the L-S coupling induced \dot{a} is a function of Ω and ω , as shown in the appendix, we have

$$\dot{x}_2 = \frac{\dot{a}_p \sin i}{c} = \frac{\dot{a}}{a} x . \quad (63)$$

Therefore, the L-S coupling induced \dot{x} is given by

$$\dot{x} = \dot{x}_1 + \dot{x}_2 = -x \dot{\Omega} \sin \lambda_{LJ} \sin \Omega \cot i + \frac{\dot{a}}{a} x . \quad (64)$$

By Eq.(64) we have

$$\ddot{x} = \dot{x}_1 \left(\frac{\ddot{\Omega}}{\dot{\Omega}} + \dot{\Omega} \cot \Omega + \frac{\dot{\lambda}_{LJ} \cos \lambda_{LJ}}{\sin \lambda_{LJ}} \right) + x \frac{\ddot{a}a - \dot{a}^2}{a^2} + \dot{x}_2 \frac{\dot{a}}{a} . \quad (65)$$

Notice that $\dot{\Omega}$ and $\ddot{\Omega}$ can be obtained by Eq.(48). Considering $\lambda_{LJ} \ll 1$ and by Eq.(59), Eq.(60), the observational advance of precession of periastron is given (Smarr & Blandford 1976, Wex & Kopeikin 1999),

$$\omega^{\text{obs}} = \omega + \Omega - \lambda_{LJ} \cot i \sin \Omega . \quad (66)$$

Therefore, we have

$$\dot{\omega}^{\text{obs}} = \dot{\omega} + \dot{\Omega} - \dot{\lambda}_{LJ} \cot i \sin \Omega . \quad (67)$$

If $\dot{\omega}$ and $\dot{\Omega}$ are caused only by the S-L coupling effect ($H = H_S$), then $\dot{\omega}$ is given by Eq.(56). If we consider all terms of the Hamiltonian, as given by Eq.(2), then $\dot{\omega}$ should include $\dot{\omega}^{GR}$, the advance of precession of periastron predicted by general relativity, which caused by H_{1PN} and H_{2PN} . In such case $\dot{\omega}$ in Eq.(67) is replaced by $\dot{\omega}^{GR} + \dot{\omega}$. Thus Eq.(67) can be written as

$$\dot{\omega}^{\text{obs}} = \dot{\omega}^{GR} + \dot{\omega}^S . \quad (68)$$

where

$$\dot{\omega}^S = \dot{\omega} + \dot{\Omega} - \dot{\lambda}_{LJ} \cot i \sin \Omega . \quad (69)$$

Notice that $\dot{\omega}^S$ is a function of time due to $\dot{\Omega}$, $\dot{\omega}$ and λ_{LJ} are function of time, as shown in Eq.(49), Eq.(56) and Eq.(93) respectively. Whereas, $\dot{\omega}^{GR}$ is a constant as shown in Eq.(8).

For a binary pulsar system with negligibly small eccentricity, the effect of the variation in the advance of periastron, ω , is absorbed by the redefinition of the orbital frequency. As discussed by Kopeikin (1996), $\omega^{\text{obs}} + A_e(u)$ is given

$$\omega^{\text{obs}} + A_e(u) = \omega_0 + \frac{2\pi}{P_b}(t - t_0) , \quad (70)$$

where $A_e(u)$ is the true anomaly, related to the eccentric anomaly, u , by the transcendental equation, ω_0 is the orbital phase at the initial epoch t_0 .

At the time interval, $\delta t = (t - t_0)$, there is a corresponding $\delta\omega^{\text{obs}}$ which causes a corresponding δP_b at the right hand side of Eq.(70), therefore, P_b is a function of time. Thus we have

$$\delta\omega^{\text{obs}} + A_e(u) = \frac{2\pi}{P_b}\delta t . \quad (71)$$

Write $1/P_b$ in Taylor series, we have

$$\frac{1}{P_b} = \frac{1}{P_b(t_0)} - \frac{\dot{P}_b(t_0)\delta t}{P_b^2(t_0)} + \dots \quad (72)$$

Considering $A_e(u) = 2\pi\delta t/P_b(t_0)$ and by Eq.(71), Eq.(72) obtains,

$$\delta\dot{\omega}^{\text{obs}} = -\frac{2\pi\dot{P}_b}{P_b^2}\delta t . \quad (73)$$

Since $\dot{\omega}^S$ is a function of time, whereas $\dot{\omega}^{GR} = \text{const}$, then we have $\ddot{\omega}^{\text{obs}} = \ddot{\omega}^S$ by Eq.(68). Assume $F = \dot{\omega}^S$, and write it in Taylor series as: $F = F_0 + \dot{F}\delta t + \frac{1}{2}\ddot{F}\delta t^2$, obtains $\delta F = \delta\dot{\omega}^S \approx \dot{F}\delta t = \ddot{\omega}^S\delta t$. Therefore, $\delta\dot{\omega}^{\text{obs}}$ of Eq.(73) becomes $\delta\dot{\omega}^S = \ddot{\omega}^S\delta t$, from which Eq.(73) can be written as

$$\dot{P}_b = -\frac{\ddot{\omega}^S P_b^2}{2\pi} . \quad (74)$$

By Eq.(74), the derivatives of P_b can be obtained,

$$\ddot{P}_b = \frac{2\dot{P}_b^2}{P_b} - \frac{P_b^2}{2\pi} \frac{d^3\omega^S}{dt^3} \approx -\frac{P_b^2}{2\pi} \frac{d^3\omega^S}{dt^3} , \quad (75)$$

$$\frac{d^3 P_b}{dt^3} \approx -\frac{P_b^2}{2\pi} \frac{d^4\omega^S}{dt^4} . \quad (76)$$

6. Comparison of three different S-L coupling induced $\dot{\omega}^{\text{obs}}$ and \dot{P}_b

6.1. Discrepancy between Wex & Kopeikin and this paper

Sect 4 calculates the S-L coupling induced change of orbital elements of a binary system directly in the J-coordinate system (in which z axis is along $\hat{\mathbf{J}}$ and $x - y$ plane is the invariance plane). And Sect 5 transform the effects in J-coordinate system to the observer's coordinate system, and obtains \dot{x} , $\dot{\omega}^{\text{obs}}$ and \dot{P}_b . In which $\dot{\omega}^{\text{obs}}$ is equivalent to the definition of Wex & Kopeikin (1999) as shown in Fig 2a.

By Eq(56) the $\dot{\omega}$ can be 1.5 PN (or $\dot{\omega} = 0$ in 1PN), thus by Eq(69) the the S-L coupling induced precession of periastron, $\dot{\omega}^S$, becomes

$$\dot{\omega}^S \approx \dot{\Omega} - \dot{\lambda}_{LJ} \cot i \sin \Omega . \quad (77)$$

Eq(77) is the result corresponding to 9 degrees of freedom, and $\dot{\omega}^S$ is 1PN. On the other hand, Wex & Kopeikin (1999), rewrite BO's orbital precession velocity, Eq(12) in the J-coordinate system, and then obtain \dot{x} , $\dot{\omega}^{\text{obs}}$ in observer's coordinate system.

However the difference is that for Wex & Kopeikin (1999), all the results in the J-coordinate system is calculated in to 12 degrees of freedom. In such case J in Eq(56) is replaced by S , thus the first term at the right hand side of Eq(56) is 0.5PN smaller than that of the second term. Therefore $\dot{\omega}$ can be represented by the second term at the right hand side of Eq(56), which is 1PN. By Eq(69), and considering $\dot{\Omega} - \dot{\Omega} \cos \lambda_{LJ} \sim 1.5PN$ ($\lambda_{LJ} \ll 1$), we have

$$\dot{\omega}^S \approx -\dot{\lambda}_{LJ} \cot i \sin \Omega . \quad (78)$$

Since $\dot{\lambda}_{LJ} \sim \dot{\Omega}$, as shown in Eq(92) and Eq(93), $\dot{\omega}^S$ is also 1PN. From which we also have significant $\ddot{\omega}^S$ (1PN), and therefore, significant derivative of P_b by Eq(74)-Eq(76). IN other words Wex &

Kopeikin's (ω of Eq(59) Wex & Kopeikin (1999)) actually corresponding significant variabilities, such as $\dot{\omega}^S$ and \dot{P}_b .

So Eq(77) and Eq(78) both correspond to significant $\dot{\omega}^S$ and \dot{P}_b . However there is an obvious discrepancy between Eq(77) and Eq(78), that is in Eq(78), $\dot{\omega}^S \rightarrow 0$ when $i \rightarrow \pi/2$. Whereas, Eq(77) doesn't have such a relation. Therefore, the validity of Wex & Kopeikin (1999) and this paper can be tested by binary pulsar systems with orbital inclination, $i \rightarrow \pi/2$ (edge on).

If a binary pulsar system with $i \rightarrow \pi/2$ still has significant \dot{P}_b (1PN), then Eq(78) corresponding to Wex & Kopeikin (1999) is not supported, otherwise Eq(77) corresponding to this paper is not supported.

The discrepancy between Eq(77) and Eq(78) is due to the discrepancy on $\dot{\omega}$, which is caused by different degrees of freedom used in this paper and Wex & Kopeikin (1999).

Eq(77) and Eq(78) have important property in common, that is $\dot{\omega}^S$ (and therefore, $\dot{\omega}^{obs}$) is obtained by the transformation from the J-coordinate system to the observer's coordinate system, in which all the three triads are at rest to "an observer" in SSB.

6.2. Discrepancy between Damour & Schäfer and Wex & Kopeikin

Damour & Schäfer (1988) express the orbital precession velocity as,

$$\dot{\Omega}_S = \frac{d\Omega_S}{dt} \mathbf{K}_0 + \frac{d\omega}{dt} \mathbf{k} + \frac{di}{dt} \mathbf{i}, \quad (79)$$

where \mathbf{K}_0 unit vector along is line of sight, which defines the third vector of a reference triad (\mathbf{I}_0 , \mathbf{J}_0 , \mathbf{K}_0), where \mathbf{I}_0 - \mathbf{J}_0 corresponds to plane of the sky. And the triad of the orbit is (\mathbf{i} , \mathbf{j} , \mathbf{k}), in which \mathbf{k} corresponds to $\hat{\mathbf{L}}$. \mathbf{i} is the nodal vector determined by the intersection of the two planes (notice that it is different from the scalar, i , which represents the orbital inclination), as shown in Fig 2b. By Eq(79), and the relations between the reference triad, components of $\dot{\Omega}_S$ are obtained (Damour & Schäfer 1988).

$$\frac{d\omega}{dt} = \frac{1}{\sin^2 i} [\dot{\Omega}_S \cdot \mathbf{k} - \dot{\Omega}_S \cdot \mathbf{K}_0 \cos i], \quad (80)$$

$$\frac{d\Omega_S}{dt} = \frac{1}{\sin^2 i} [\dot{\Omega}_S \cdot \mathbf{K}_0 - \dot{\Omega}_S \cdot \mathbf{k} \cos i], \quad (81)$$

$$\frac{di}{dt} = \dot{\Omega}_S \cdot \mathbf{i}. \quad (82)$$

The S-L coupling induced $\dot{\omega}$ given by Eq(80) is $\dot{\omega} \sim \dot{\Omega}_S \sim 1.5\text{PN}$. Therefore, Damour & Schäfer (1988) predict insignificant $\dot{\omega}$ ($\dot{\omega}^S$) which is much smaller than 1PN, and therefore, the corresponding \dot{P}_b is also insignificant.

Thus it seems strange that Damour & Schäfer (1988) and Wex & Kopeikin (1999) start from same orbital precession velocity given by Eq(12), but predict different observational effect.

This is because $\dot{\omega}^S$ of Wex & Kopeikin is calculated in a coordinate system with axes (x', y', z') at rest to "an observer" at SSB as shown in Fig 2a. Whereas, $\dot{\omega}$ ($\dot{\omega}^S$) of Damour & Schäfer is calculated in a coordinate system with triad $(\mathbf{K}_0, \mathbf{k}, \mathbf{i})$, which is not at rest to "an observer" at SSB as shown in Fig 2b. Obviously \mathbf{i} (point A), which is the intersection of the plane of the sky and the orbital plane of a binary system, is not static in the coordinate system (x', y', z') of Wex & Kopeikin (1999), so is \mathbf{k} .

If Damour & Schäfer's $\dot{\omega}$ is also calculated in the coordinate system as that of Wex & Kopeikin, then Eq(80) reduces to Eq(78).

Therefore, the discrepancy between Damour & Schäfer (1988) and Wex & Kopeikin (1999) is the different coordinate systems chosen in the calculation of S-L coupling induced effects of a binary system. Whereas, the discrepancy between Wex & Kopeikin (1999) and this paper is different degree of freedom used in the calculation of equation of motion of a binary system. The relationship of the three kinds of S-L coupling effects is shown in Fig 4.

7. Confrontation with observation

The precise timing measurement on two typical binary pulsars provide evidence on whether $\dot{\omega}^S$ and \dot{P}_b is 1PN or 1.5PN, but it still difficult to distinguish which 1PN effect is valid, Wex & Kopeikin (1999) or this paper.

The orbital motion causes a delay of $T = \mathbf{r}_1 \cdot \mathbf{K}_0/c = r_1(t) \sin \omega^{\text{obs}}(t) \sin i(t)/c$ in the pulse arrival time, where \mathbf{r} is the pulsar position vector and \mathbf{K}_0 is the unit vector of the line of sight. The residual $\delta T = \mathbf{r}_1 \cdot \mathbf{K}_0/c - (\mathbf{r}_1 \cdot \mathbf{K}_0/c)_K$ of the time delay compared with the Keplerian value is of interest (Lai et al. (1995)). Averaging over one orbit $r \approx a$, and in the case $t \ll 1/|\dot{\omega}^{\text{obs}}|$, the S-L coupling induced residual is,

$$\begin{aligned} \delta T &= \frac{a_p}{c} \cos i \frac{di}{dt} t \sin \omega^{\text{obs}} + \frac{\dot{a}_p \sin i}{c} t \sin \omega^{\text{obs}} + \frac{a_p \sin i}{c} \dot{\omega}^{\text{obs}} t \cos \omega^{\text{obs}} \\ &= \dot{x}_1 t \sin \omega^{\text{obs}} + \frac{\dot{a}}{a} t \sin \omega^{\text{obs}} + \dot{\omega}^{\text{obs}} t \cos \omega^{\text{obs}}. \end{aligned} \quad (83)$$

By Eq.(89), we have $\dot{a}/a \sim J/a^3 \sim \dot{\omega}^{\text{obs}}$, therefore, the second and third term at the right hand side of Eq.(83) cannot be distinguished in the current treatment of pulsar timing. In other words, the effect of \dot{a} can be absorbed by $\dot{\omega}^{\text{obs}}$.

7.1. PSR J2051-0827

As discussed above, the second term at the right hand side of Eq.(64) can be absorbed by $\dot{\omega}^{\text{obs}}$, therefore $\dot{x} \approx \dot{x}_1$, and by Eq.(62), we have

$$\dot{\Omega} = -\frac{\dot{x}}{x} \frac{\tan i}{\sin \lambda_{LJ} \sin \Omega_0} = -\frac{di}{dt} \frac{1}{\sin \lambda_{LJ} \sin \Omega_0}. \quad (84)$$

According to optical observations, the system is likely to be moderately inclined with an inclination angle $i \sim 40^\circ$ (Stappers et al. 2001). By the measured results of $x = 0.045\text{ s}$, $\dot{x} = -23(3) \times 10^{-14}$ (Doroshenko et al. 2001), and by assuming $\sin \lambda_{LJ} \sin \Omega_0 = 2 \times 10^{-3}$, Eq.(84) can be written in magnitude,

$$\dot{\Omega} = \left(\frac{\dot{x}}{2.3 \times 10^{-13}} \right) \left(\frac{x}{0.045} \right)^{-1} \left(\frac{\tan i}{\tan 40^\circ} \right) \left(\frac{\sin \lambda_{LJ} \sin \Omega_0}{2 \times 10^{-3}} \right)^{-1} \sim 2 \times 10^{-9} (\text{s}^{-1}) . \quad (85)$$

In the following estimation of this section all values are absolute values. By Eq.(56), we can assume $\ddot{\omega}^S \sim (\dot{\omega}^S)^2 \sim \dot{\Omega}^2 \approx 4 \times 10^{-18}$. Usually $\ddot{\omega}^S$ can vary in a large range, i.e., $\ddot{\omega}^S > (\dot{\omega}^S)^2$, depending on different combination of parameters, such as binary parameters, magnitude and orientation of S_1 and S_2 . In this paper we assume that $\ddot{\omega}^S \sim (\dot{\omega}^S)^2$. Thus from Eq.(74) we have,

$$\dot{P}_b = \frac{1}{2\pi} \left(\frac{\ddot{\omega}^S}{4 \times 10^{-18}} \right) \left(\frac{P_b}{0.099\text{ d}} \right)^2 \sim 5 \times 10^{-11} (\text{ss}^{-1}) . \quad (86)$$

By Eq.(69), we can estimate $d^3\omega^S/dt^3 \sim \dot{\Omega}^3 \approx 8 \times 10^{-27} \text{ s}^{-3}$, similarly, we can estimate $d^4\omega^S/dt^4 \sim \dot{\Omega}^4 \approx 16 \times 10^{-36} \text{ s}^{-4}$.

Therefore, by Eq.(75) and Eq.(76) we have $\ddot{P}_b \sim 9 \times 10^{-20} \text{ s}^{-1}$ and $d^3P_b/dt^3 \sim 2 \times 10^{-28} \text{ s}^{-2}$. By Eq.(64) and Eq.(65), $\ddot{x}/\dot{x} \sim \dot{\Omega} \sim 2 \times 10^{-9} \text{ s}^{-1}$, which is consistent with observation as shown in Table 2.

Therefore, once \dot{x} is in agreement with the observation, the corresponding $\dot{\omega}^S$ can make the derivatives of P_b be consistent with observation as shown in Table 2. Whereas, the effect derived from Damour & Schäfer's equation cannot explain the significant derivatives of P_b .

7.2. PSR J1713+0747

By the measured parameters, $x = 32.3\text{ s}$, $|\dot{x}| = 5(12) \times 10^{-15}$, $i = 70^\circ$ (Camilo et al. 1994), and by assuming $\sin \lambda_{LJ} \sin \Omega_0 = 1 \times 10^{-4}$, then in magnitude we have,

$$\dot{\Omega} = \left(\frac{\dot{x}}{5 \times 10^{-15}} \right) \left(\frac{x}{32.3} \right)^{-1} \left(\frac{\tan i}{\tan 70^\circ} \right) \left(\frac{\sin \lambda_{LJ} \sin \Omega_0}{1 \times 10^{-4}} \right)^{-1} \sim 4 \times 10^{-12} (\text{s}^{-1}) , \quad (87)$$

similarly we have,

$$\dot{P}_b = \frac{1}{2\pi} \left(\frac{\ddot{\omega}^S}{16 \times 10^{-26}} \right) \left(\frac{P_b}{67.8\text{ d}} \right)^2 \sim 1 \times 10^{-10} (\text{ss}^{-1}) . \quad (88)$$

The comparison of observational and predicted variabilities are shown Table 3, which are well consistent. Notice that \dot{x}^{obs} and \dot{P}_b^{obs} measured in these three typical binary pulsars cannot be interpreted by the gravitational radiation induced \dot{x} and \dot{P}_b , since they are 3 or 4 order of magnitude smaller than those of the observational ones.

8. Discussion and conclusion

BO and AK's orbital precession velocity has been treated as equivalent, since BO and AK's $\dot{\mathbf{L}}$ give equivalent value, as shown in Eq.(9) and Eq.(18) respectively. Actually Eq.(9) and Eq.(18) correspond to two different orbital precession velocities, Eq.(12) and Eq.(19) respectively, which is caused by different physical conditions imposed on the calculation. AK's satisfies the triangle constraint and BO's violates it. The one that satisfies the triangle constraint corresponds to 9 degree of freedom for a binary system, whereas, the one that violates it corresponds to 12 degree of freedom.

The discrepancy in physics results discrepancy in observation. Eq.(12) and Eq.(19) correspond to different Ω and ω (as defined in Fig.2), and since observational effect depends on Ω and ω instead of $\dot{\mathbf{L}}$, therefore, the equivalent value in $\dot{\mathbf{L}}$ doesn't mean that the predicted observational effects are identical. Concretely, BO and AK give same Ω , but different ω . And by Eq.(66) and Eq.(67), the observed advance of precession of periastron depends on both Ω and ω , thus BO and AK must correspond to different observational effects.

In the calculation of Sect 4 and Sect 5, we can see the influence of the degree of freedom and physical constraint on the results of equation of motion, perturbation and observational effects.

The S-L coupling induced precession of orbit can cause an additional time delay to the time of arrivals (TOAs), which can be absorbed by the orbital period. And since the additional time delay itself is a function of time, therefore orbital period change, \dot{P}_b , appears. Actually \dot{P}_b corresponds to $\ddot{\omega}^S$ as shown in Eq.(74), which cannot be absorbed by $\dot{\omega}^{GR}$ ($\dot{\omega}^S$ can be absorbed by $\dot{\omega}^{GR}$). Therefore, the higher order of derivatives of orbital period provide good chance to test different models. The observation of \dot{P}_b , \ddot{P}_b and d^3P_b/dt^3 on PSR J 2051-0827 supports significant S-L coupling induced effects.

This paper for the first time points out that Wex & Kopeikin's expression in 1999 actually corresponds to significant $\dot{\omega}^S$ and \dot{P}_b , however it is not equivalent to the significant $\dot{\omega}^S$ and \dot{P}_b given by this paper. Specific binary pulsars with orbital inclination $i \rightarrow \pi/2$ may provide chance to test the validity of the results corresponding to Wex & Kopeikin (1999) and that of this paper.

I thank T. Huang for help in clarifying the theoretical part of this paper. I thank R.N. Manchester for his help in understanding pulsar timing measurement. I thank T. Lu for useful comments during this work. I thank W.T. Ni and C.M. Xu for useful suggestions in the presentation of this paper. I thank E.K. Hu, A. Rüdiger, K.S. Cheng, N.S. Zhong, and Z.G. Dai for continuous encouragement and help. I also thank Y. Li, Z.X. Yu, C.M. Zhang, L. Zhang, Z. Li, H. Zhang, S.Y. Liu, X.N. Lou, X.S. Wan for useful discussions.

9. Appendix

By $\tilde{S} = \mathbf{a}_{so} \cdot \hat{\mathbf{n}}$ and $T = \mathbf{a}_{so} \cdot \hat{\mathbf{t}}$, $\frac{d\Omega}{dt}$ and $\frac{d\omega}{dt}$ have been given by Eq.(48), Eq.(49), Eq.(54), and Eq.(56), following the standard procedure for computing perturbations of orbital elements Roy ((1991)). Similarly, four other elements can be given:

$$\frac{da}{dt} = \frac{2}{n\sqrt{1-e^2}}(\tilde{S}e \sin f + \frac{p\tilde{T}}{r}) , \quad (89)$$

$$\frac{de}{dt} = \frac{\sqrt{1-e^2}}{na}[\tilde{S} \sin f + \tilde{T}(\cos E + \cos f)] , \quad (90)$$

$$\langle \frac{de}{dt} \rangle = \frac{4\sigma_1 J e h}{(1-e^2)^{3/2} a^3 p} (P_x Q_y - P_y Q_x) , \quad (91)$$

$$\frac{d\lambda_{LJ}}{dt} = \frac{\tilde{W} r \cos(\omega + f)}{na^2 \sqrt{1-e^2}} \frac{1}{\sin \lambda_{LJ}} , \quad (92)$$

$$\begin{aligned} \langle \frac{d\lambda_{LJ}}{dt} \rangle = & \frac{3 \cos \lambda_{LJ}}{2a^3(1-e^2)^{3/2} \sin \lambda_{LJ}} (P_z \cos \omega + Q_x \sin \omega) [(P_y Q_z - P_z Q_y)(S_x \sigma_1 + S_{2x} \sigma_2) \\ & + (P_z Q_x - P_x Q_z)(S_y \sigma_1 + S_{2y} \sigma_2) + (P_x Q_y - P_y Q_x)(S_z \sigma_1 + S_{2z} \sigma_2)] , \end{aligned} \quad (93)$$

$$\frac{d\epsilon}{dt} = \frac{e^2}{1 + \sqrt{1-e^2}} \frac{d\varpi}{dt} + 2 \frac{d\Omega}{dt} (1-e^2)^{1/2} (\sin^2 \frac{\lambda_{LJ}}{2}) - \frac{2r\tilde{S}}{na^2} , \quad (94)$$

where $\frac{d\varpi}{dt} = \frac{d\omega'}{dt} + 2 \frac{d\Omega}{dt} (\sin^2 \frac{\lambda_{LJ}}{2})$.

$$\begin{aligned} \langle \frac{d\epsilon}{dt} \rangle = & \frac{e^2}{1 + \sqrt{1-e^2}} \langle \frac{d\varpi}{dt} \rangle + 2 \langle \frac{d\Omega}{dt} \rangle (1-e^2)^{1/2} (\sin^2 \frac{\lambda_{LJ}}{2}) \\ & - \frac{4\sigma_1 J h}{a^3(1-e^2)p} (P_x Q_y - P_y Q_x) . \end{aligned} \quad (95)$$

REFERENCES

Apostolatos,T.A., Cutler, C., Sussman,J.J. Thorne,K.S., 1994, Phys. Rev. D, **49**, 6274–6297 .

Barker,B.M., O'Connell, R.F., 1975, Phys. Rev. D, **12**, 329–335.

Camilo, F., Foster, R.S., Wolszczan, A., 1994, Astrophys. J. **437**, L39–L42 .

Damour, T., Schäfer, G., 1988 IL Nuovo Cimento, **101B**, 127 .

Doroshenko,O., Löhmer, O., Kramer, M., Jessner, A., Wielebinski,R., Lyne,A.G., Lange, Ch., 2001, Astro-Astrophys, **379**, 579–588 .

Hamilton, A.J.S. Sarazin, C.L., 1982, MNRAS **198**, 59–70 .

Kidder, L.E., 1995, Phys. Rev. D, **52**, 821–847.

Kopeikin, S.M., 1996, Astrophys. J. **467**, L93–L95.

Lai, D., Bildsten, L., Kaspi,V., 1995, Astrophys. J. **452**, 819–824 .

Liu, L., 1993, Method in Celestial Mechanics, Nanjing University Press

Roy, A.E., 1991, Orbital motion, Adam Hilger

Smarr, L.L.,Blandford, R.D., 1976, Astrophys. J. **207**, 574–588.

Stappers, B.W. , Van Kerkwijk,M.H., Bell, J.F., Kulkarni, S.R., 2001, Astrophys. J. **548**, L183–L186 .

Wex, N., Kopeikin, S.M., 1999, Astrophys. J. **514**, 388.

Yi, Z.H., 1993, Essential Celestial Mechanics, Nanjing University Press

Table 1: Comparison of S-L coupling induced variabilities given by different authors

	DS (1988)	WK (1999)	This paper	evidence
$\dot{\Omega}$ in J-co		1PN	1PN	
$\dot{\omega}$ in J-co		1PN	1.5PN	
$\dot{\omega}^S$	$\sim \dot{\Omega}_S$ (of Eq.(12))	$-\dot{\lambda}_{LJ} \cot i \sin \Omega$	$\dot{\Omega} - \dot{\lambda}_{LJ} \cot i \sin \Omega$	
$\dot{\omega}^{\text{obs}}$	$\dot{\omega}^{GR} + 1.5\text{PN}$	$\dot{\omega}^{GR} + 1\text{PN}$	$\dot{\omega}^{GR} + 1\text{PN}$	
\dot{P}_b	\dot{P}_b^{GR}	$ \dot{P}_b^{\text{obs}} \gg \dot{P}_b^{GR} $	$ \dot{P}_b^{\text{obs}} \gg \dot{P}_b^{GR} $	$ \dot{P}_b^{\text{obs}} \gg \dot{P}_b^{GR} $
when $i \rightarrow \pi/2$		$\dot{P}_b^{\text{obs}} \rightarrow \dot{P}_b^{GR}$	$ \dot{P}_b^{\text{obs}} \gg \dot{P}_b^{GR} $	

J-co represents J-coordinate system, \dot{P}_b^{GR} represents orbital period change due to gravitational radiation predicted by General Relativity. $\dot{\Omega}_S$ is given by Eq.(12) which is 1.5PN, whereas, $\dot{\Omega}$ and $\dot{\lambda}_{LJ}$ are 1PN, as given by Eq.(49) and Eq.(92) respectively.

Table 2: Measured parameters compared with the geodetic precession induced ones in PSR J2051–0827

observation	WK & this paper
$\dot{x}^{\text{obs}} \approx -23(3) \times 10^{-14}$	$\dot{x} = \dot{x}^{\text{obs}}$
$(\ddot{x}/\dot{x})^{\text{obs}} \leq -3.0 \times 10^{-9} \text{s}^{-1}$	$ \ddot{x}/\dot{x} \approx 2 \times 10^{-9} \text{s}^{-1}$
$\dot{P}_b^{\text{obs}} = -15.5(8) \times 10^{-12}$	$ \dot{P}_b = \frac{\dot{\omega}^S P_b^2}{2\pi} \sim 5 \times 10^{-11}$
$\ddot{P}_b^{\text{obs}} = 2.1(3) \times 10^{-20} \text{s}^{-1}$	$ \ddot{P}_b = \frac{P_b^2}{2\pi} \frac{d^3 \omega^S}{dt^3} \sim 9 \times 10^{-20} \text{s}^{-1}$
$\frac{d^3 P_b^{\text{obs}}}{dt^3} = 3.6(6) \times 10^{-28} \text{s}^{-2}$	$ \frac{d^3 P_b}{dt^3} = \frac{P_b^2}{2\pi} \frac{d^4 \omega^S}{dt^4} \sim 2 \times 10^{-28} \text{s}^{-2}$

Table 3: Measured parameters compared with the geodetic precession induced ones in PSR J1713+0747

observation	WK & this paper
$ \dot{x} ^{\text{obs}} = 5(12) \times 10^{-15}$	$\dot{x} = \dot{x}^{\text{obs}}$
$\dot{P}_b^{\text{obs}} = 1(29) \times 10^{-11}$	$ \dot{P}_b = \frac{\dot{\omega}^S P_b^2}{2\pi} \sim 1 \times 10^{-10}$

Fig. 1.— In 1PN, the scenario of motion of a binary pulsar system can be described as the rotation of the plane determined by \mathbf{L} , \mathbf{S} around the fixed axis, \mathbf{J} . η_L and η_S are precession phases of \mathbf{L} and \mathbf{S} in the J-coordinate system respectively.

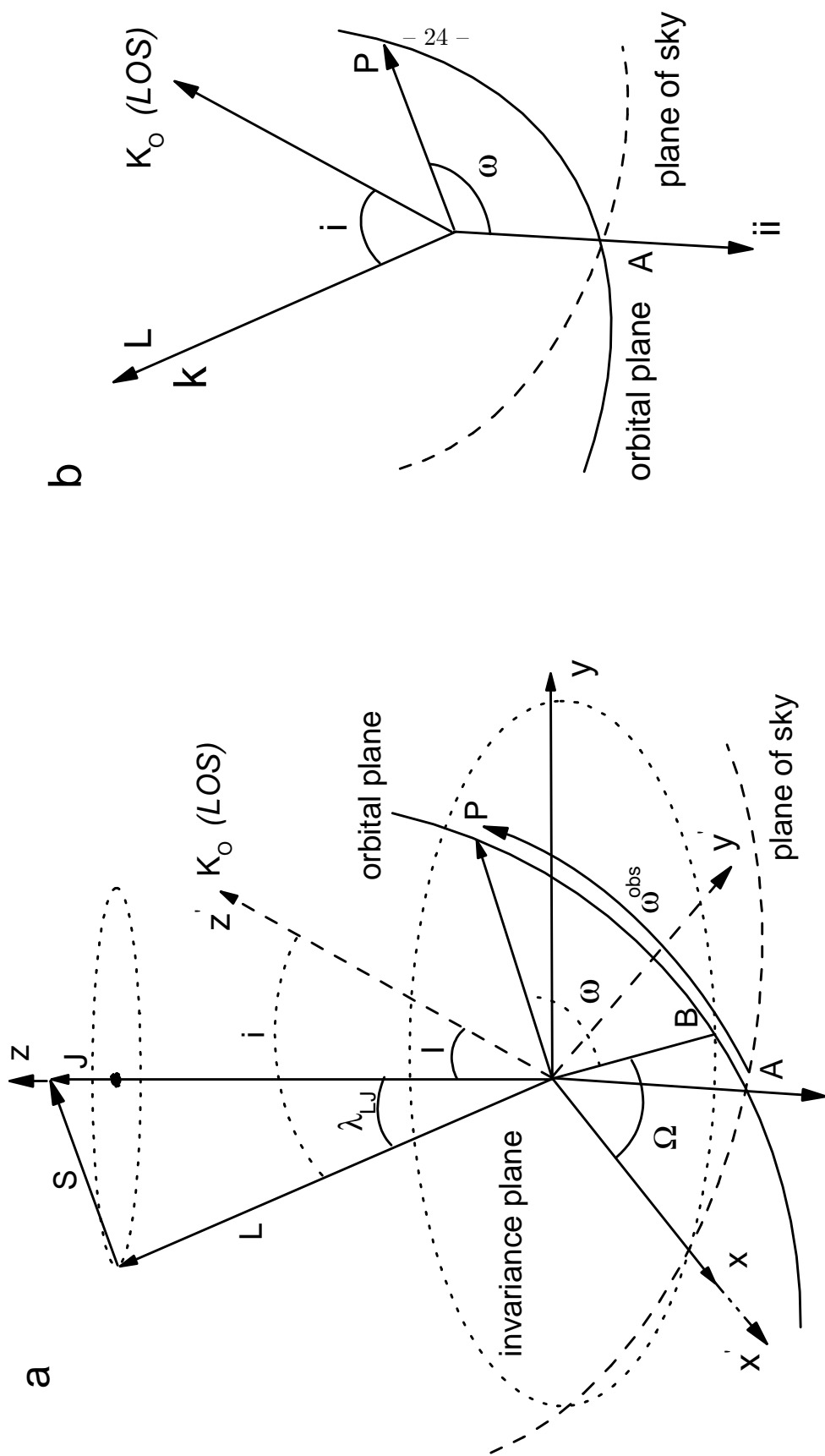


Fig. 2.— Fig 2a: binary geometry and definitions of angles of Wex & Kopeikin (1999) and this paper. The invariable plane (x-y), as represented by the dotted ellipse, is perpendicular to the total angular momentum, \mathbf{J} . The inclination of the orbital plane with respect to the invariable

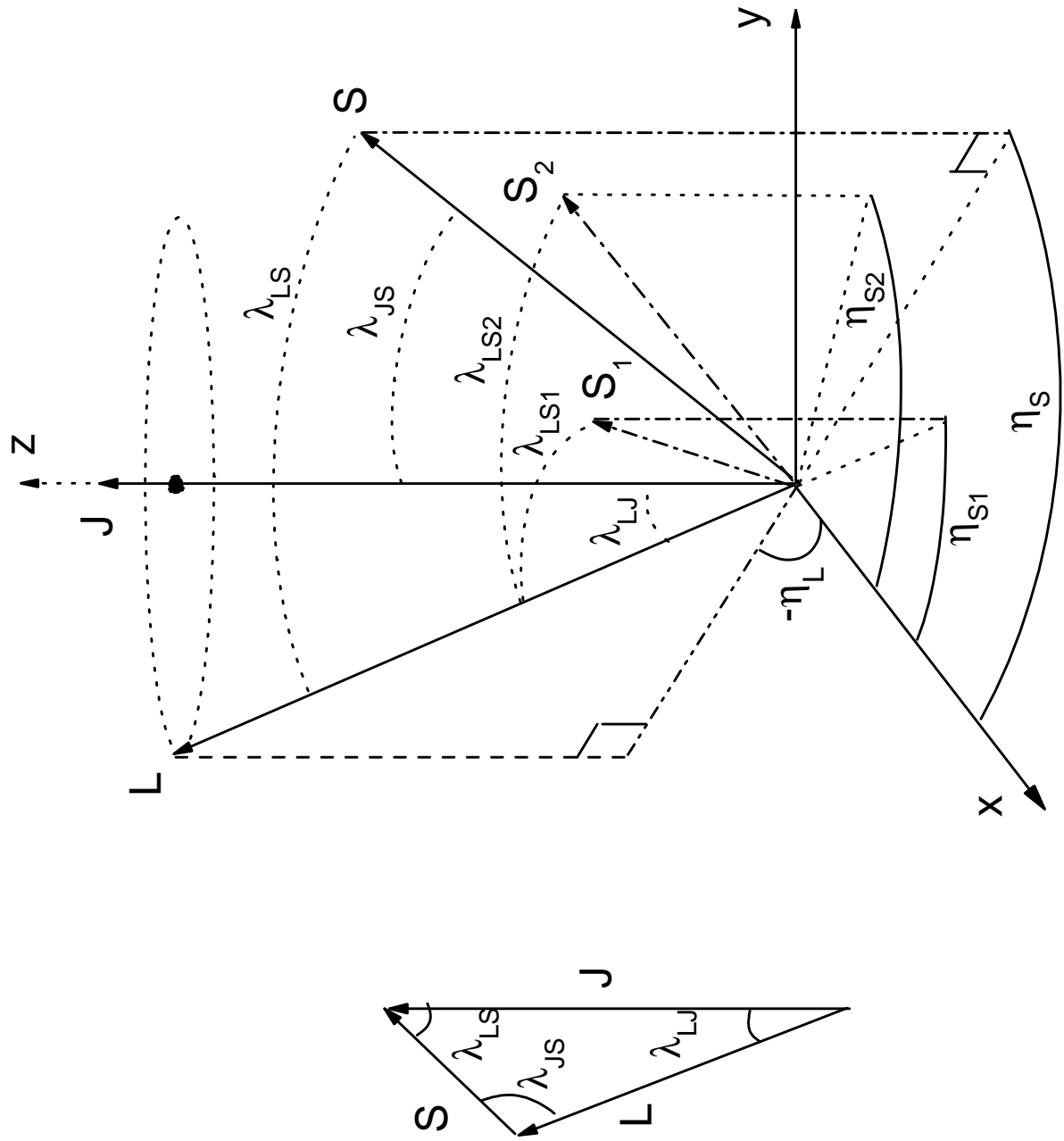


Fig. 3.— Angles and orientation conventions relating vectors \mathbf{S} , \mathbf{L} and \mathbf{J} to the coordinate system. x - y is the invariance plane, η_{S1} , η_{S2} , η_s and η_L are precession phases of \mathbf{S}_1 , \mathbf{S}_2 , \mathbf{S} and \mathbf{L} , respectively.

Fig. 4.— The relationship of the three kinds of S-L coupling induced orbital effects.

